https://doi.org/10.5194/os-2019-50
Preprint. Discussion started: 11 June 2019

Ocean Science
Discussions
Open Access
EGU

Downscaling sea-level rise effects on tides and sediment dynamics in tidal bays

Long Jiang[1], Theo Gerkema[1], Déborah Idier[2], Aimée B. A. Slangen[1], and Karline Soetaert[1]

[1] NIOZ Royal Netherlands Institute for Sea Research, Department of Estuarine and Delta Systems, and Utrecht University, P.O. Box 140, 4400 AC Yerseke, The Netherlands.
[2] BRGM, 3, avenue C. Guillemin, 45060 Orléans cedex 2, France.

Correspondence to: Long Jiang (long.jiang@nioz.nl)

Abstract. Sea-level rise (SLR) not only increases the threat of coastal flooding, but also may change tidal regimes in estuaries and coastal bays. To investigate such nearshore tidal responses to SLR, a hydrodynamic model of the European Shelf is downscaled to a model of a Dutch coastal bay (the Eastern Scheldt) and forced by SLR scenarios ranging from 0 to 2 m. The results indicate that SLR induces larger increases in tidal amplitude and stronger nonlinear tidal distortion in the bay compared to the adjacent shelf sea. Under SLR, the basin shifts from a mixed flood- and ebb-dominant state to complete ebb-dominance, causing enhanced sediment export and accelerated loss of tidal flats. In this case study, we find that local impacts of SLR can be highly spatially-varying and nonlinear depending on basin geometry. Our model downscaling approach is widely applicable for establishing local SLR projections in estuaries and coastal bays.

1 Introduction

Sea-level rise (SLR) poses an increasing flood risk on global shorelines (FitzGerald et al., 2008; Haigh et al., 2014). In addition to the direct increment in water levels, SLR induces changes in global and regional tidal regimes (Devlin et al., 2017; Pelling et al., 2013b; Pickering et al., 2017). Understanding these tidal changes is an imperative step towards projecting future water levels and designing shoreline protection works (Katsman et al., 2011). Shifts in estuarine and coastal tidal regimes including tidal amplitude, residual currents, and tidal asymmetry can potentially modify sediment transport, which further influences the fate of salt marsh accretion and shoreline morphology (Chernetsky et al., 2011; Nnafie et al., 2014; van Goor et al., 2003). Furthermore, in estuaries and embayments, changes in tidal mixing and currents are expected to have implications for salt intrusion, nutrient transport, primary production and other ecosystem functions (Nienhuis and Smaal, 1994). Therefore, in order to mitigate the SLR hazards in estuaries and coastal bays, it is of high priority to study the SLR impact on tides.

SLR-induced tidal changes in estuaries and embayments are more complex than in the open ocean and shelf seas (Holleman and Stacey, 2014). Tidal waves propagating in nearshore regions are strongly deformed via factors like shoaling, damping, and reflection (resonance). As these processes respond to SLR to various extents, this triggers spatially heterogeneous modifications in tidal regimes (e.g., Pickering et al., 2012; Carless et al., 2016). Therefore, tidal responses to

https://doi.org/10.5194/os-2019-50
Preprint. Discussion started: 11 June 2019

SLR vary among and within systems (Holleman and Stacey, 2014; Pelling and Green, 2014). For example, with SLR, the tidal amplitude may increase due to reduced friction (Arns et al., 2015; Idier et al., 2017) or decrease as a consequence of enhanced dissipation in the newly inundated areas (Ross et al., 2017). Overtides and tidal asymmetry can also be modulated distinctly among estuaries, with ramifications for residual sediment transport and morphodynamic development (Gräwe et al., 2014; van der Wegen, 2013). In shallow flood-dominant estuaries with a high tidal amplitude/basin depth ratio (a/h >0.3), tidal asymmetry is likely to weaken with SLR if increases in a cannot keep up with h, reducing the seaward bedload transport (Friedrichs and Aubrey, 1988). In contrast, in ebb-dominant bays with vast areas of intertidal flats, SLR may causes a sharp decline in intertidal flats and transition to flood-dominance, favoring sediment import (Brown and Davies, 2010). Thus, given the various responses in different types of basins, tidal impacts of SLR should be assessed on a system- or site-specific basis.

Although challenging, tidal changes due to SLR have been modeled in both idealized and realistic estuaries and bays (e.g., Du et al., 2018; Holleman and Stacey, 2014; Hong and Shen, 2012; Pelling et al., 2013b). Generally, studies with idealized (simplified) basin shapes cannot fully address the spatially nonuniform shoaling, reflection, and damping in realistic systems. Furthermore, in most modeling studies, SLR is prescribed by simply increasing the surface elevation at the open boundary, without considering tidal changes in the shelf seas that may propagate into estuaries/bays. In fact, before entering estuaries, tidal waves on the shelf are significantly modified in amplitude and phase or distorted (Idier et al., 2017; Pickering et al., 2017). Chernetsky et al. (2010) found that the externally generated overtides play a key role in the sediment dynamics within an estuary. This underlines the necessity of coupling the coastal and shelf processes with the dynamics of land-locked water bodies for SLR assessments.

Here, we present a case study with regional SLR projections driving a hydrodynamic model of the European Shelf, which is then downscaled for the Eastern Scheldt, a Dutch tidal bay adjacent to the North Sea (Fig. 1). We investigate the SLR impacts on the local tidal dynamics and the implications for residual sediment transport. This study also seeks broad applicability of the model downscaling method when predicting SLR influences in other estuaries and coastal bays.

2 The study site

The Eastern Scheldt (ES, Dutch name: Oosterschelde) is a well-mixed tidal bay on the southwestern coast of the Netherlands (Fig. 1). Because of the limited freshwater input, the semidiurnal-dominant tides control the water renewal and material transport in ES (Jiang et al., 2019). A storm surge barrier (hereafter referred to as “barrier”, Fig. 1) constructed at its mouth in the late 1980s reduced the tidal prism and amplitude by ~30% and 13%, respectively. As a result, the tidal flat and salt marsh areas and landward supply of sediments, nutrients, seston, and chlorophyll sharply declined, and the residence time was doubled (Nienhuis and Smaal, 1994). Due to a decreased sediment source, erosion of tidal flats is ongoing, disturbing ecosystem services in the bay (Vroon, 1994). Since the construction of the barrier, tides have not been substantially changed by changing bed morphology of the basin (de Pater, 2012).

https://doi.org/10.5194/os-2019-50
Preprint. Discussion started: 11 June 2019

SLR at the Dutch coast may exceed 1 m between 2000 and 2100 under a high greenhouse gas emission scenario (Vermeersen et al., 2018). With SLR, the tidal amplitude (mostly semidiurnal components) and tidal volume in the southern North Sea, adjacent to ES, are projected to increase mainly due to reduced friction (Idier et al., 2017; Pelling et al., 2013a; Pickering et al., 2012). As a result of the increased water depth on the European shelf, tidal wave propagation can be accelerated, leading to earlier arrival of semidiurnal tidal waves, i.e., reduced semidiurnal phases, in the southern North Sea (Idier et al., 2017). The SLR-induced increased tidal amplitude may reverse some of the above post-barrier trends and highlight the local need of exploring the tidal responses to SLR in ES.

3 Methods

We adopted the hydrodynamic model MARS (Model for Applications at Regional Scale, Lazure and Dumas, 2008) to model tides on the European Shelf at a horizontal resolution of 2 km, and, in a downscaling, GETM (General Estuarine Transport Model, www.getm.eu) to model tides in ES at a resolution of 300 m (Fig. 1). The description and setup of these two models are introduced by Idier et al. (2017) and Jiang et al. (2019), respectively. This section therefore focuses on the model downscaling setup, SLR scenarios, and model calibration.

MARS was forced with 14 major tidal components (Mf, Mm, Msqm, Mtm, O1, P1, Q1, K1, M2, K2, 2N2, N2, S2, and M4) from a global tide model FES2004 (Lyard et al., 2006). The MARS domain (Fig. 1) extends to deep waters (> 200 m) so that the SLR-induced changes in tidal components at its open boundary is minimal. The year 2009 was used as the baseline scenario, and the observed water elevation and tidal components from 16 tide gauges are well reproduced by MARS in 2009 (Idier et al., 2017).

The SLR scenarios were implemented in MARS by uniformly increasing the open-boundary water level in the baseline scenario. Using the water level data from a regional SLR projection model (Slangen et al., 2014), Idier et al. (2017) also tested a scenario with nonuniform open-boundary SLR and found insignificant differences of tides from the uniform scenarios in the southern North Sea. Thus, only the MARS results with uniform SLR scenarios are used for downscaling to the ES model. The SLR scenarios used for the MARS model are 0.25 m, 0.5 m, 0.75 m, 1.0 m, 1.5 m, and 2.0 m. Local projections for Vlissingen (Fig. 1) considering regional sea-level contributions (Slangen et al., 2014) were used to estimate when these idealized SLR scenarios might occur. In the MARS domain, most low-lying land within 2 m height above the present sea level is located on the eastern shore of the North Sea, i.e., Belgium, the Netherlands, Germany, and Denmark (www.flood.firetree.net/), where the coastlines are well protected from flooding (Pelling and Green, 2014). Hence, the SLR scenarios were conducted without flooding of these shorelines in both MARS and GETM. Atmospheric forcing was not included in the model setup.

GETM was used to downscale MARS to the ES region in a one-way coupling mode. The Flather open boundary (Flather, 1988) was applied in GETM, in which the gravity-wave radiation condition requires the prescribing both water elevation and current velocity as boundary forcing. In the baseline and every SLR scenario, these two variables in the

https://doi.org/10.5194/os-2019-50
Preprint. Discussion started: 11 June 2019

vicinity of the GETM open boundary (Fig. 1) were extracted from MARS output every 15 min and linearly interpolated to each GETM open boundary node (255 nodes totally, Jiang et al., 2019). Every scenario was run for one year and the time series of modeled tidal elevation and currents were decomposed with the T_TIDE toolbox (Pawlowicz et al., 2002) to extract the major components for all grid cells excluding the tidal flats. The modeled water level and major tidal components in the baseline scenario were compared with observations (accessible from www.rijkswaterstaat.nl/water) at three stations inside ES (Fig. 1, Section 4.1).

Tidal asymmetry was estimated using the phase difference between the M2 and M4 currents following Friedrichs and Aubrey (1988): a positive, zero, and negative value of $\cos(2\phi_{UM2} - \phi_{UM4})$ indicates flood-dominance, symmetric tide, and ebb-dominance, respectively, where ϕ_{UM2} and ϕ_{UM4} are the phases of M2 and M4 current velocity, respectively. Assuming a negligible settling time lag between the local suspended sediment concentration and currents (Ridderinkhof, 1997), Gräwe et al. (2014) proposed an analytical quantity Q (kg m^{-1} s^{-1}, Eq. (1)) as the depth-integrated residual sediment transport including both bedload and suspended transport, especially in systems with relatively weak stratification and estuarine circulation, such as ES (Burchard et al., 2013).

$$\mathrm{Q} = \frac{3\alpha\kappa_v}{4w_s^2} U_{M2}^2 U_{M4} \cos(2\phi_{UM2} - \phi_{UM4}) \quad (1)$$

In Eq. (1), α is the sediment erosion parameter (kg s m^{-4}), κ_v is the vertical diffusion coefficient (m^2 s^{-1}), w_s is the settling velocity (m s^{-1}), and U_{M2} and U_{M4} are the magnitude of the M2 and M4 current velocity (m s^{-1}), respectively. To estimate Q, we applied the model computed M2 and M4 velocity and phase, along with the typical values of α (0.001), κ_v (0.01), and w_s (0.001) suggested by Burchard et al. (2013) and Gräwe et al. (2014) for weakly stratified estuaries and the North Sea. Q is then used to estimate the directional changes in residual sediment transport in different SLR scenarios. This saves substantial computational costs compared to a sophisticated sediment transport model.

4 Results

4.1 The baseline scenario

Our modeled water elevation in the baseline scenario (SLR = 0) matches well with the observed water level at tide gauges with the overall correlation coefficients > 0.95 and normalized standard deviations (Taylor, 2001) < 0.1 (dimensionless). For example, Figs. 2a and 2b shows the high agreement between simulated and observed water elevation during days 175-185, a period with relatively weak winds given that the coupled models were run without atmospheric forcing. The tidal range (TR) increases from 2.5 m to 3.4 m from the mouth to head (Fig. 3a), illustrating the convergence property of ES. In addition to the water level, the model captures the observed magnitude and phase of M2 and its major overtide M4 with relatively small errors (Fig. 2).

As the dominant component in ES, the M2 magnitude captures most of the TR spatial pattern and it takes ~30 min (phase difference ~15°) for the semidiurnal tidal wave to propagate from the western to eastern side (Fig. 4c). The sharply

https://doi.org/10.5194/os-2019-50
Preprint. Discussion started: 11 June 2019

reduced water depth caused by the barrier at the mouth significantly weakens the tidal amplitude and delays the propagation of tidal waves (Figs. 3 and 4). This discontinuity in the tidal amplitude and phase between the North Sea and ES is consistent with previous observations (Vroon, 1994). The barrier also changes tidal asymmetry, with ebb- and flood-dominance on its seaward and landward sides creating a zone of sediment divergence (Fig. 5a). Tidal asymmetry also differs inside the bay: near the eastern part vast areas of tidal flats provoke a shift to ebb-dominance, while the rest of the basin stays flood-dominant (Fig. 5a). The modeled boundary of ebb- and flood-dominance indicates sediment convergence in the central basin (Fig. 5a), which agrees with the area of shallower bed levels (Fig. 1). Hence, our model captures the variations of observed water elevation as well as the main tidal patterns in the system.

4.2 SLR effects on the tidal amplitude and phase

In the absence of sediment deposition and erosion, the tidal flats will be gradually inundated by the increasing sea level at an accelerated pace (Fig. 6a). With SLR, TR increases almost uniformly within ES, taking the 1 m SLR scenario as an example (Fig. 3b). The average TR over the entire bay increases nearly proportionally to SLR according to the linear regression $TR = 0.337 * SLR + 2.93$ ($r^2 > 0.995$), all in metres, indicating a 11.5% increase in TR per metre SLR (Fig. 6a). This rate is six time faster than that in the adjacent North Sea, where $TR = 0.0544 * SLR + 3.12$ ($r^2 > 0.995$, Fig. 6a). It should be noted that TR declined by ~0.35 m after the construction of the barrier, so that, based on our estimation, the pre-barrier magnitude will be restored at around 1 m SLR, which may occur by the end of the 21st century (Fig. 6a). Since SLR does not change the total basin area in our simulation not allowing flooding of the coastlines, a larger tidal range indicates increased tidal prism with SLR. Therefore, tidal currents are strengthened in most of the basin (Fig. 7).

The increase of M2, S2, and M4 amplitudes is also proportional to SLR, with a slope of 0.157, 0.056, and 0.029 m/m SLR ($r^2 > 0.995$). These increasing magnitudes per metre SLR account for 11.3%, 15.7%, and 40.4% of the M2, S2, and M4 magnitude in the baseline scenario, respectively. The spatial patterns of the semidiurnal components M2 and S2 are similar to that of the overall TR, and accordingly they are more sensitive to SLR inside the bay compared to outside (e.g., Fig. 4b). In contrast, under SLR the M4 amplitude decreases outside, while it increases inside ES (Fig. 4f). Compared to the baseline scenario, the M4 amplitude increases (40.4% per metre SLR) much faster than TR and the main semidiurnal components, indicative of the non-linear effects involved in its generation.

Tidal waves in shallow waters propagate at a speed of $\sqrt{gh}$, which therefore increases under SLR as water depth h increases. In addition, the decline in bottom friction favors faster wave propagation. Consequently, the phases of semidiurnal components decrease with SLR, with a larger change in the bay compared to the coastal sea (e.g., Fig. 4d). In contrast, the M4 phase varies in a nonuniform and non-linear way, implying strong modifications of shallow-water tides under SLR (Fig. 4h).

https://doi.org/10.5194/os-2019-50
Preprint. Discussion started: 11 June 2019

4.3 SLR-induced shifts in tidal asymmetry and implications for sediment transport

The different responses of M2 and M4 under SLR conditions change the tidal asymmetry in ES. The entire bay shifts from a mixed ebb- and flood-dominance (Fig. 5a) to an increasingly ebb-dominant state (Fig. 5b). The switch of the entire bay occurs at SLR below 0.25 m, as indicated by the M2-M4 phase difference (Fig. 6b). In the scenario with 1 m SLR, the flood-dominant western part becomes ebb-dominant, while the ebb-dominance in the eastern part is enhanced; in contrast, the M2-M4 phase difference in the adjacent North Sea is relatively insensitive to SLR (Fig. 5b).

The quantity Q is used to estimate the combined effects of tidal current velocity and asymmetry on residual sediment transport. With both tidal currents and ebb-dominance strengthened by SLR, the absolute value of Q is amplified, especially when the SLR is below 1 m (Fig. 6b and 7). According to our estimates, the residual transport more than doubles with 1 m SLR and nearly triples with 2 m SLR (Fig. 6b). The increased sediment export under these scenarios is mainly through channels where tidal currents are strong (Fig. 7a). Our results illustrate that despite the fact that SLR can restore the pre-barrier TR, this will not be accompanied by sufficient net sediment import as was in the past (Mulder and Louters, 1994). It is therefore likely that future SLR will amplify the already ongoing erosion of tidal flats in ES.

5 Discussion and summary

This case study shows how future SLR may change the tidal regime and residual sediment transport in a tidal bay. Understanding the tidal responses to SLR is fundamental to anticipating any ecosystem shifts and adjusting management strategies in global estuaries and bays. For instance, our results imply that at least an extra 30 cm needs to be accounted for in dike construction to effectively protect the inland against the high water at spring tides for 1 m SLR in ES, similarly as reported for other coastal systems (Arns et al. 2015; Devlin et al., 2017). As TR increases under SLR, the turnover time, an indicator of water renewal efficiency, is significantly shortened in most parts of the basin (Fig. 8). This will put the system under a greater influence of the North Sea, likely increasing import of nutrients and organic matters and carrying capacity of shellfish culture (Jiang et al., 2019). In many other nearshore systems, tides changed as a result of SLR were also found to alter the ecosystem functions (Bhuiyan e al., 2012; Hong and Shen, 2012).

One intriguing finding in our study is a much stronger tidal response to SLR in the bay compared to the coastal sea (Fig. 6a). This is not a consequence of enhanced resonance. The quarter-wavelength resonance period of our system ($T = 4L/\sqrt{gh}$, where L is the basin length, see e.g., Gerkema, 2019) in the baseline scenario is 5.3 hours. The Helmholtz resonance does not apply to the ES because of the along-channel semidiurnal phase difference (~15º, 30 min, Fig. 4c). Moreover, the Helmholtz resonance period ($T_H = 2\pi\sqrt{AL_b/(gBH)}$, where A is the basin area and L_b, B, and H are length, width, and depth of the channel connecting the bay and North Sea; Gerkema, 2019) for ES is no longer than 2.4 hours. Both T and T_H are much shorter than the semidiurnal tidal period. With h and H increased with SLR and L, L_b, *and* B unchanged, T and T_H will decrease and shift further away from semidiurnal resonance. With the resonance impacts ruled out, reduced

https://doi.org/10.5194/os-2019-50
Preprint. Discussion started: 11 June 2019

frictional damping increases the semidiurnal tidal amplitude by 0.03-0.05 m/m SLR in the study region, as suggested by Idier et al. (2017). Besides friction, the amplified TR by SLR likely results from the features in basin geometry, including narrowing, shoaling, and the presence of the barrier. For example, within 5 km on the seaward side of the barrier, water depth does not differ greatly from the adjacent North Sea, but the cross-sectional area is significantly reduced; consequently, TR increases faster than in the North Sea. Into the barrier, while basin width is rather constant, the average water depth is much shallower than outside so that TR is further amplified (Fig. 3b). This finding underlines the vulnerability of nearshore systems, mainly coastal bays and estuaries, to future SLR. Hence, more attention should be directed to SLR projections on estuarine and embayment scales.

Another major finding of this study is the SLR-induced changes in tidal asymmetry and the potential effects on sediment transport. Tidal distortion and asymmetry result from interactions between basin geometry and shallow-water tidal waves (Speer and Aubrey, 1985). Shallow waters with a high a/h ratio are usually flood-dominant because of a stronger frictional damping during ebb, while an extensive intertidal area flanking deep channels can slow down flood currents and generate ebb-dominance (Friedrichs and Aubrey, 1988). With SLR, the water depth increases, and tidal flats diminish. These two processes render the system to a less flood- and ebb-dominant state, respectively; the shift of tidal asymmetry depends on these two competing effects (Friedrichs et al., 1990). Our study finds ES to become ebb-dominant with SLR. In contrast, the Ems estuary may obtain a stronger flood-dominant signal (Chernetsky et al., 2010), whereas tidal asymmetry is insensitive to SLR in the Ria de Aveiro lagoon (Lopes and Dias, 2015). Both suspended and bedload sediment transport are strongly associated with tidal asymmetry, especially in weakly stratified estuaries, and are important to the long-term basin geomorphology (Burchard et al., 2013; van Maren et al., 2004). Our results reveal an increased sediment export with SLR, detrimental to shoreline protection and salt marsh accretion.

Although our results are not generic to global estuaries and bays, this study shows the complicated interaction between basin geometry and tides and pinpoints the urgency of understanding estuarine tidal responses under changing SLR conditions. To this end, our case study highlights the following aspects to be fully considered.

Firstly, tidal responses to SLR can vary from system to system, and comparative studies are much needed. Because of the spatially varying coastline and bathymetry, shallow-water tides react to friction, shoaling, and reflection (including resonance characteristics) to different extents among and within systems under SLR (e.g., Fig. 6a; Carless et al., 2016; Idier et al., 2017). Thus, compared to shelf-sea models, estuarine models with refined spatial resolution are required to capture the detailed features of bathymetry and coastlines, and hence nearshore tidal distortion.

Secondly, in addition to water height, SLR-induced tidal variations in the shelf seas have significant impacts on estuarine/embayment dynamics. Tides in shelf seas exhibit nonlinear and nonuniform responses to SLR (Idier et al., 2017; Pickering et al., 2012), and these effects may amplify in estuaries and bays. Nevertheless, most previous studies into SLR effects on estuaries simply increased the water level, neglecting changes in the tidal characteristics at their coastal boundary (e.g., Hong and Shen, 2012; Holleman and Stacey, 2014). Based on our further examination of a scenario raising the open-boundary water height only, such simplification overestimates (underestimates) the TR in ES (North Sea) by 9 (4) cm for 1

https://doi.org/10.5194/os-2019-50
Preprint. Discussion started: 11 June 2019

m SLR and completely misses the reduction of tidal phases. Without variations in externally generated M4 tides, calculation of estuarine tidal asymmetry and sediment transport can produce different results (Chernetsky et al., 2010). Therefore, given the relatively coarse resolution of shelf-sea models in estuaries and the inability of estuarine models to resolve the shelf-sea tidal variations due to SLR, model downscaling is essential in examining nearshore SLR impacts.

Thirdly, nearshore studies should be combined with regional SLR projections to steer efficient shoreline management strategies. Despite large uncertainties associated with emission scenarios and sea-level contributions (Slangen et al., 2014), regional SLR projections provide specific timelines for tidal changes and set the time window for required management actions in the coming decades. For example, the shift to ebb-dominance will likely occur before 2050, while nourishment of intertidal flats will be continuously needed well beyond 2100 (Fig. 6). Shoreline defense against SLR ranges from hard measures that prevent flooding, such as levees and dikes, as in the Netherlands, to soft measures which allow flooding, such as using marshes and newly inundated areas for dissipating tidal waves, for instance in parts of the Chesapeake Bay (Holleman and Stacey, 2014). Including these coastal defense measures in numerical models can significantly affect the sensitivity of tides to SLR (Idier et al., 2017; Ross et al., 2017). In our model setup, intertidal flats around channels were allowed to drown, while the shorelines with dikes were not (Fig. 1). Clearly, our results might change if the actual shoreline defense were to be implemented differently.

It should be noted that our downscaled model does not account for winds, the gravitational force, and the potential changes in basin geomorphology. According to recent studies, wind climate can also contribute significantly to long-term variability of regional water elevation (Arns et al., 2015; Gerkema and Duran-Matute, 2017). Density-driven flow can also dominate local transport processes (Schulz and Gerkema, 2018). While tides in ES were not strongly affected by bathymetric changes in the past decades (de Pater, 2012), it would be interesting to investigate the interaction between SLR and basin morphology by implementing a geomorphology component into our model. Finally, downscaling in our study is based on a one-way model coupling without accounting for feedbacks (e.g., dissipation and reflection) from the bay to shelf seas. It could prove worthwhile to investigate how increasing details in embayment geometry can affect the SLR projections and associated tidal changes on the shelf, e.g. due to the radiation of M4 from the basin into the adjacent sea.

Code and data availability

The source code for the MARS and GETM model used in this study are available at https://wwz.ifremer.fr/mars3d/ and https://getm.eu/. Research data is archived on 4TU.Research Data (https://data.4tu.nl/) with the doi https://doi.org/10.4121/uuid:c6753aa0-d501-4cbe-9476-a2833d47bfc6.

https://doi.org/10.5194/os-2019-50
Preprint. Discussion started: 11 June 2019

Author contributions

LJ ran the GETM simulations, analyzed the results, and initiated the writing of the manuscript. TG and KS provided guidance and important insights into data interpretation. DI ran the MARS simulation. ABAS conducted the regional SLR projection. All authors participated in the writing and editing of the manuscript.

Competing interests.

No competing interests are present.

Acknowledgments

This work was supported by the collaborative framework of Utrecht University and Royal Netherlands Institute for Sea Research.

References

Arns, A., Wahl, T., Dangendorf, S., and Jensen, J.: The impact of sea level rise on storm surge water levels in the northern part of the German Bight, Coast. Eng., 96, 118–131, https://doi.org/10.1016/j.coastaleng.2014.12.002, 2015.

Bhuiyan, M. J. A. N., and Dutta, D.: Assessing impacts of sea level rise on river salinity in the Gorai river network, Bangladesh, Estuar. Coast. Shelf Sci., 96, 219–227, https://doi.org/10.1016/j.ecss.2011.11.005, 2012.

Brown, J. M., and Davies, A. G.: Flood/ebb tidal asymmetry in a shallow sandy estuary and the impact on net sand transport, Geomorphology, 114, 431-439, https://doi.org/10.1016/j.geomorph.2009.08.006, 2010.

Burchard, H., Schuttelaars, H. M., and Geyer, W. R.: Residual sediment fluxes in weakly-to-periodically stratified estuaries and tidal inlets, J. Phys. Oceanogr., 43, 1841–1861, https://doi.org/10.1175/JPO-D-12-0231.1, 2013.

Carless, S. J., Green, J. M., Pelling, H. E., and Wilmes, S. B.: Effects of future sea-level rise on tidal processes on the Patagonian Shelf, J. Mar. Syst., 163, 113–124, https://doi.org/10.1016/j.jmarsys.2016.07.007, 2016.

Chernetsky, A. S., Schuttelaars, H. M., and Talke, S. A.: The effect of tidal asymmetry and temporal settling lag on sediment trapping in tidal estuaries, Ocean Dynam., 60, 1219–1241, https://doi.org/10.1007/s10236-010-0329-8, 2010.

de Pater, P. D.: Effect of removal of the Oosterschelde storm surge barrier. MSc. thesis. Delft University of Technology, 2012.

Devlin, A. T., Jay, D. A., Talke, S. A., Zaron, E. D., Pan, J., and Lin, H.: Coupling of sea level and tidal range changes, with implications for future water levels, Sci. Rep., 7, 17021, https://doi.org/10.1038/s41598-017-17056-z, 2017.

https://doi.org/10.5194/os-2019-50
Preprint. Discussion started: 11 June 2019

Du, J., Shen, J., Zhang, Y. J., Ye, F., Liu, Z., Wang, Z., Wang, Y. P., Yu, X., Sisson, M., and Wang, H. V.: Tidal response to sea-level rise in different types of estuaries: The importance of length, bathymetry, and geometry, Geophys. Res. Lett., 45, 227–235, https://doi.org/10.1002/2017GL075963, 2018.

FitzGerald, D. M., Fenster, M. S., Argow, B. A., and Buynevich, I. V.: Coastal impacts due to sea-level rise, Annu. Rev. Earth Planet. Sci., 36, https://doi.org/10.1146/annurev.earth.35.031306.140139, 2008.

Flather, R. A.: A numerical model investigation of tides and diurnal-period continental shelf waves along Vancouver Island, J. Phys. Oceanogr., 18(1), 115-139, https://doi.org/10.1175/1520-0485(1988)018<0115:ANMIOT>2.0.CO;2, 1988.

Friedrichs, C. T., and Aubrey, D. G.: Non-linear tidal distortion in shallow well-mixed estuaries: a synthesis. Estuar. Coast. Shelf Sci., 27, 521–545, https://doi.org/10.1016/0272-7714(88)90082-0, 1988.

Friedrichs, C. T., Aubrey, D. G., and Speer, P. E.: Impacts of relative sea-level rise on evolution of shallow estuaries, in: Residual Currents and Long-term Transport, edited by: Cheng, R. T., Springer, New York, 105–122, https://doi.org/10.1007/978-1-4613-9061-9, 1990.

Gerkema, T. (Ed.): An Introduction to Tides, Cambridge University Press, Cambridge, United Kingdom, 2019 (in press).

Gerkema, T., and Duran-Matute, M.: Interannual variability of mean sea level and its sensitivity to wind climate in an inter-tidal basin, Earth Syst. Dynam., 8, 1223–1235, https://doi.org/10.5194/esd-8-1223-2017, 2017.

Gräwe, U., Burchard, H., Müller, M., and Schuttelaars, H. M.: Seasonal variability in M2 and M4 tidal constituents and its implications for the coastal residual sediment transport, Geophys. Res. Lett., 41, 5563–5570, https://doi.org/10.1002/2014GL060517, 2014.

Haigh, I. D., Wahl, T., Rohling, E. J., Price, R. M., Pattiaratchi, C. B., Calafat, F. M., and Dangendorf, S.: Timescales for detecting a significant acceleration in sea level rise, Nat. Commun., 5, 3635, https://doi.org/10.1038/ncomms4635, 2014.

Holleman, R. C., and Stacey, M. T.: Coupling of sea level rise, tidal amplification, and inundation, J. Phys. Oceanogr., 44, 1439–1455, https://doi.org/10.1175/JPO-D-13-0214.1, 2014.

Hong, B., and Shen, J.: Responses of estuarine salinity and transport processes to potential future sea-level rise in the Chesapeake Bay, Estuar. Coast. Shelf Sci., 104, 33–45, https://doi.org/10.1016/j.ecss.2012.03.014, 2012.

Idier, D., Paris, F., Le Cozannet, G., Boulahya, F., and Dumas, F.: Sea-level rise impacts on the tides of the European Shelf, Cont. Shelf Res., 137, 56–71, https://doi.org/10.1016/j.csr.2017.01.007, 2017.

Jiang, L., Gerkema, T., Wijsman, J. W., and Soetaert, K.: Comparing physical and biological impacts on seston renewal in a tidal bay with extensive shellfish culture, J. Mar. Syst., 194, 102–110, https://doi.org/10.1016/j.jmarsys.2019.03.003, 2019.

Katsman, C. A., Sterl, A., Beersma, J. J., van den Brink, H. W., Church, J. A., Hazeleger, W., Kopp, R. E., Kroon, D., Kwadijk, J., Lammersen, R., Lowe J., Oppenheimer, M., Plag H.-P., Ridley J., von Storch, H., Vaughan, D. G., Vellinga P., Vermeersen, L. L. A., van de Wal, R. S. W., and Weisse, R.: Exploring high-end scenarios for local sea level rise to develop flood protection strategies for a low-lying delta—the Netherlands as an example, Clim. Change, 109, 617–645, https://doi.org/10.1007/s10584-011-0037-5, 2011.

Lyard, F., Lefevre, F., Letellier, T., and Francis, O.: Modelling the global ocean tides: modern insights from FES2004, Ocean Dynam., 56, 394–415, https://doi.org/10.1007/s10236-006-0086-x, 2006.

Lazure, P., and Dumas, F.: An external–internal mode coupling for a 3D hydrodynamical model for applications at regional scale (MARS), Adv. Water Resour., 31, 233–250, https://doi.org/10.1016/j.advwatres.2007.06.010, 2008.

Mulder, J. P., and Louters, T.: Fine sediments in the Oosterschelde tidal basin before and after partial closure, Hydrobiologia, 282/283, 41–56, https://doi.org/10.1007/BF00024620, 1994.

Nnafie, A., De Swart, H. E., Calvete, D., and Garnier, R.: Effects of sea level rise on the formation and drowning of shoreface-connected sand ridges, a model study, Cont. Shelf Res., 80, 32–48, https://doi.org/10.1016/j.csr.2014.02.017, 2014.

Nienhuis, P. H., and Smaal, A. C.: The Oosterschelde estuary, a case-study of a changing ecosystem: an introduction, Hydrobiologia, 282/283, 1–14, https://doi.org/10.1007/BF00024620, 1994.

Pawlowicz, R., Beardsley, B., and Lentz, S.: Classical tidal harmonic analysis including error estimates in MATLAB using T_TIDE, Comput. Geosci., 28, 929–937, https://doi.org/10.1016/S0098-3004(02)00013-4, 2002.

Pelling, H. E., and Green, J. M.: Impact of flood defences and sea-level rise on the European Shelf tidal regime, Cont. Shelf Res., 85, 96–105, https://doi.org/10.1016/j.csr.2014.04.011, 2014.

Pelling, H. E., Green, J. M., and Ward, S. L.: Modelling tides and sea-level rise: To flood or not to flood, Ocean Model., 63, 21–29, https://doi.org/10.1016/j.ocemod.2012.12.004, 2013a.

Pelling, H. E., Uehara, K., and Green, J. A. M.: The impact of rapid coastline changes and sea level rise on the tides in the Bohai Sea, China, J. Geophys. Res. Oceans, 118, 3462–3472, https://doi.org/10.1002/jgrc.20258, 2013b.

Pickering, M. D., Horsburgh, K. J., Blundell, J. R., Hirschi, J. M., Nicholls, R. J., Verlaan, M., and Wells, N. C.: The impact of future sea-level rise on the global tides, Cont. Shelf Res., 142, 50–68, https://doi.org/10.1016/j.csr.2017.02.004, 2017.

Ridderinkhof, H.: The effect of tidal asymmetries on the net transport of sediments in the Ems Dollard estuary, J. Coast. Res., 25, 41–48, 1997.

Ross, A. C., Najjar, R. G., Li, M., Lee, S. B., Zhang, F., and Liu, W.: Fingerprints of sea level rise on changing tides in the Chesapeake and Delaware Bays, J. Geophys. Res. Oceans, 122, 8102–8125, https://doi.org/10.1002/2017JC012887, 2017.

Schulz, K., and Gerkema, T.: An inversion of the estuarine circulation by sluice water discharge and its impact on suspended sediment transport, Estuar. Coast. Shelf Sci., 200, 31–40, https://doi.org/10.1016/j.ecss.2017.09.031, 2018.

Speer, P. E., and Aubrey, D. G.: A study of non-linear tidal propagation in shallow inlet/estuarine systems Part II: Theory, Estuar. Coast. Shelf Sci., 21, 207–224, https://doi.org/10.1016/0272-7714(85)90097-6, 1985.

van der Wegen, M.: Numerical modeling of the impact of sea level rise on tidal basin morphodynamics, J. Geophys. Res. Earth Surf., 118, https://doi.org/10.1002/jgrf.20034, 2013.

Taylor, K. E.: Summarizing multiple aspects of model performance in a single diagram, J. Geophys. Res. Atmos., 106(D7), 7183-7192, https://doi.org/10.1029/2000JD900719, 2001.

https://doi.org/10.5194/os-2019-50
Preprint. Discussion started: 11 June 2019

van Goor, M. A., Zitman, T. J., Wang, Z. B., and Stive, M. J. F.: Impact of sea-level rise on the morphological equilibrium state of tidal inlets, Mar. Geol., 202, 211–227, https://doi.org/10.1016/S0025-3227(03)00262-7, 2003.

van Maren, D. S., Hoekstra, P., and Hoitink, A. J. F.: Tidal flow asymmetry in the diurnal regime: bed-load transport and morphologic changes around the Red River Delta, Ocean Dynam., 54, 424–434, https://doi.org/10.1007/s10236-003-0085-0, 2004.

Vermeersen, B. L. A., Slangen, A. B. A., Gerkema, T., Baart, F., Cohen, K. M., Dangendorf, S., Duran-Matute, M., Frederikse, T., Grinsted, A., Hijma, M. P., Jevrejeva, S., Kiden, P., Kleinherenbrink, M., Meijles, E. W., Palmer, M. D., Rietbroek, R., Riva, R. E. M., Schulz, E., Slobbe, D. C., Simpson, M. J. R., Sterlini, P., Stocchi, P., van de Wal R. S. W., and van der Wegen, M.: Sea-level change in the Dutch Wadden Sea, Neth. J. Geosci., 97, 79–127, https://doi.org/10.1017/njg.2018.7, 2018.

Vroon, J.: Hydrodynamic characteristics of the Oosterschelde in recent decades, Hydrobiologia, 282/283, 17–27, https://doi.org/10.1007/BF00024618, 1994.

https://doi.org/10.5194/os-2019-50
Preprint. Discussion started: 11 June 2019

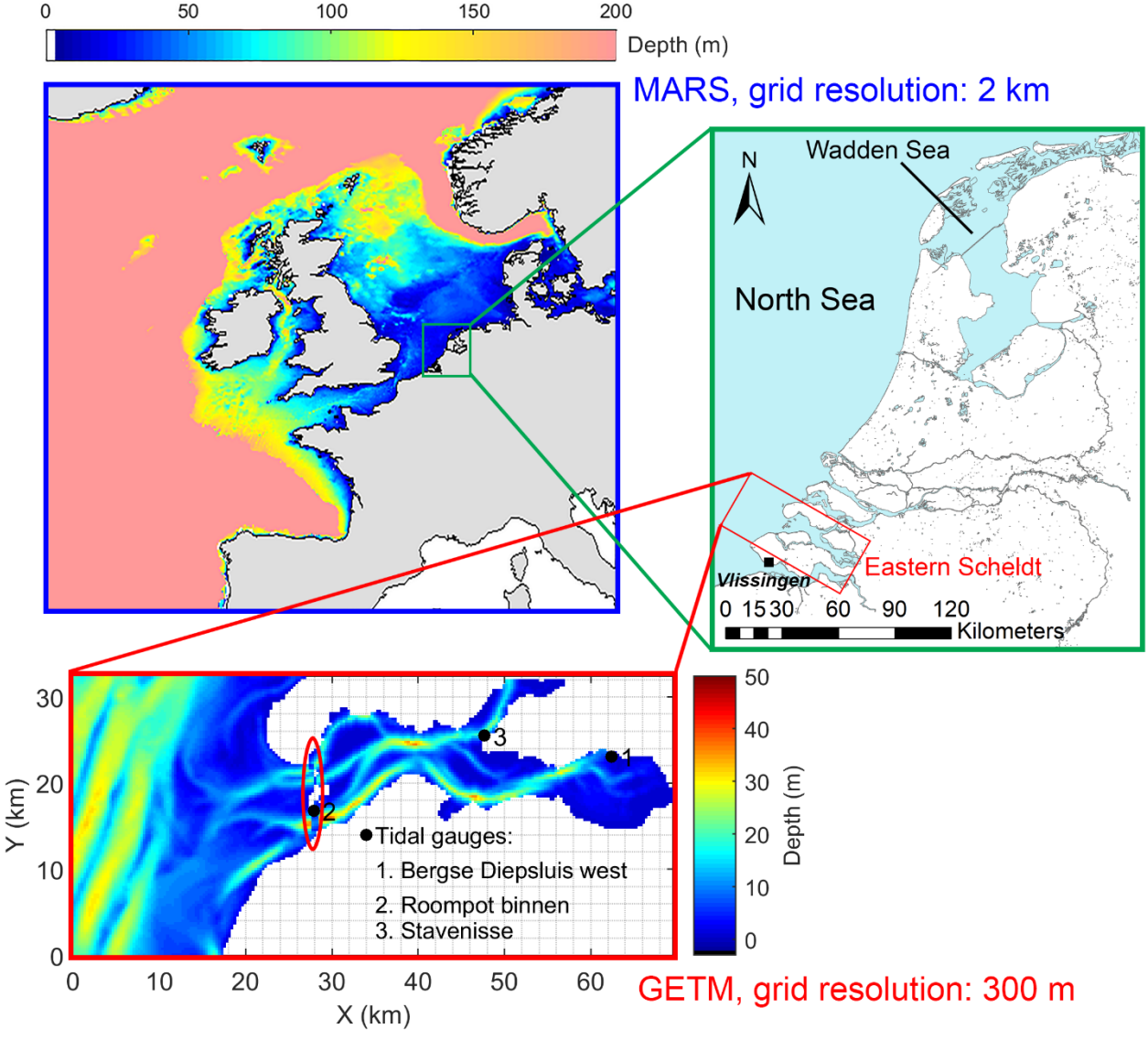

Figure 1: The study area and domains of the two hydrodynamic models representing the European Shelf (blue) and Eastern Scheldt (ES, red). The green box shows locations of ES and local SLR projection, Vlissingen, in the zoom-in map of the Netherlands. In the ES domain, tide gauges used for model calibration and the location of the storm surge barrier are marked with dots and an ellipse, respectively; white areas are land segments protected by dikes where flooding is not allowed.

https://doi.org/10.5194/os-2019-50
Preprint. Discussion started: 11 June 2019

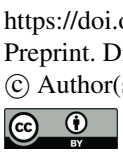

Ocean Science
Discussions
Open Access
EGU

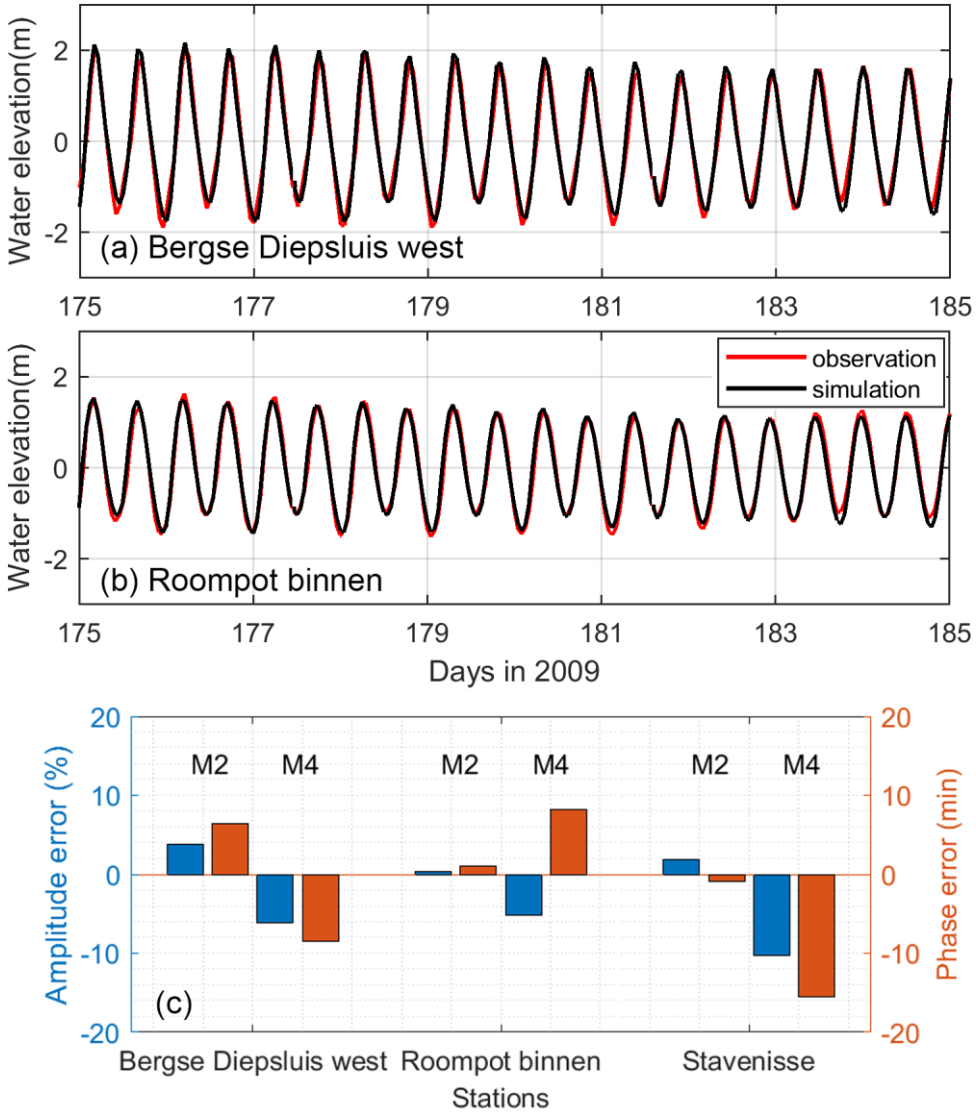

Figure 2: (a and b) Time series of modeled and observed water elevation and (c) the simulated M2 and M4 amplitude and phase errors compared to observations. See Fig. 1 for locations of data sites.

https://doi.org/10.5194/os-2019-50
Preprint. Discussion started: 11 June 2019

Ocean Science
Discussions
Open Access
EGU

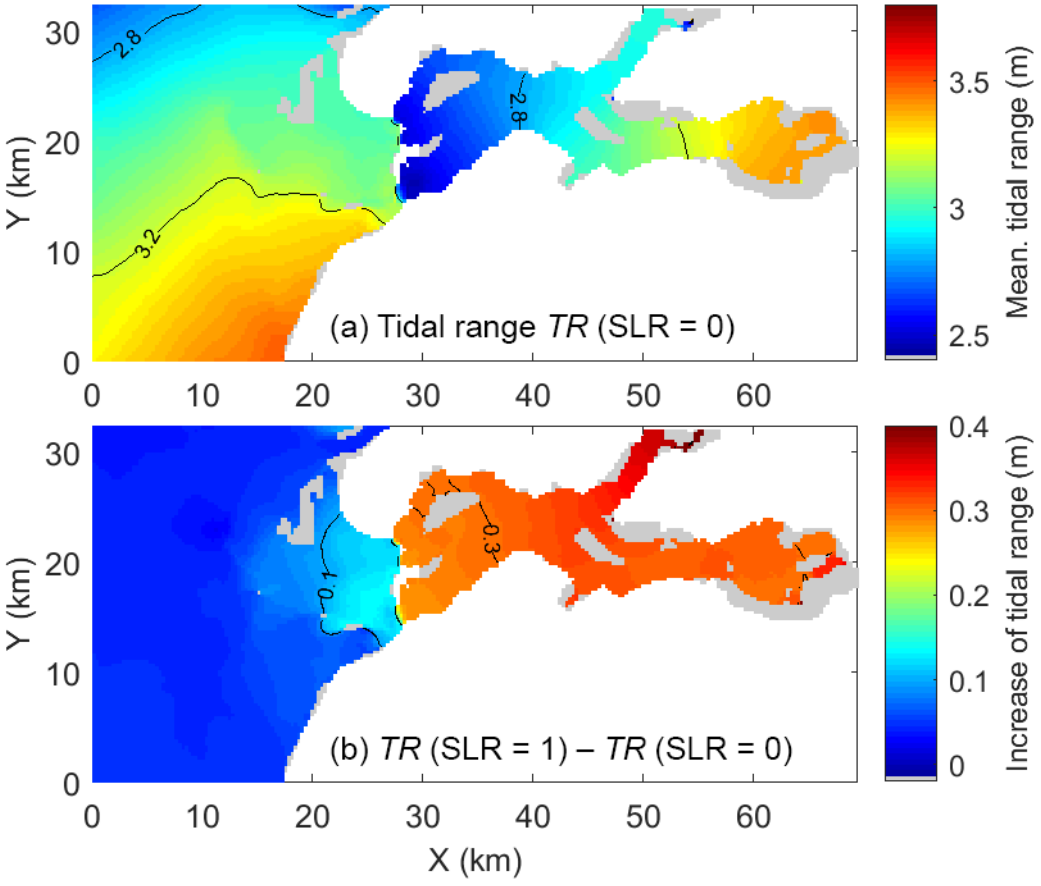

Figure 3: (a) Tidal range in the baseline scenario and (b) the difference of these two variables between the 1 m SLR and baseline scenarios. Tidal flats are shown in grey.

https://doi.org/10.5194/os-2019-50
Preprint. Discussion started: 11 June 2019

Ocean Science
Discussions
Open Access
EGU

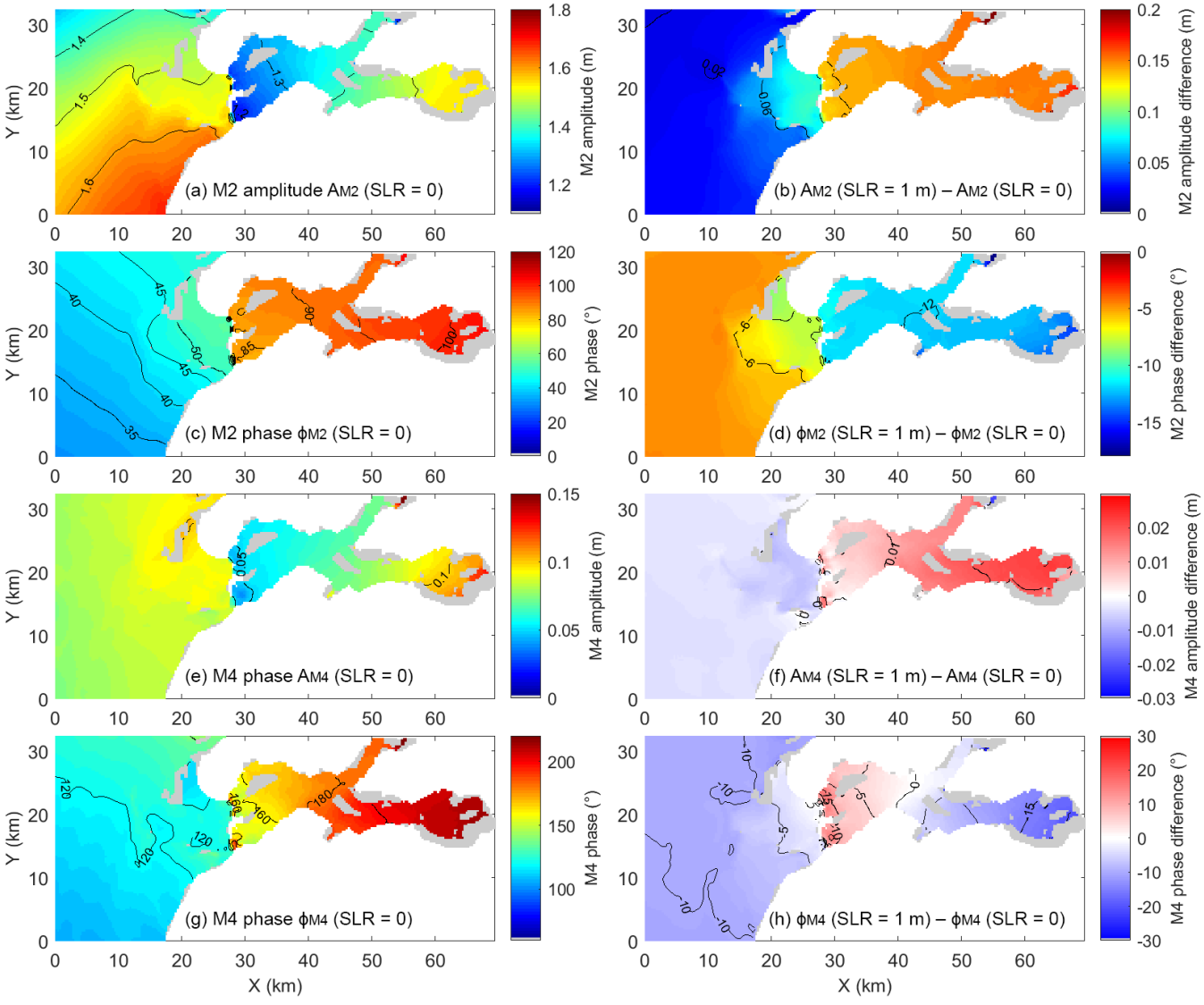

Figure 4: The M2 (a) amplitude and (c) phase and M4 (e) amplitude and (g) phase in the baseline scenario and (b, d, f and h) the difference of these variables between the 1-m-SLR and baseline scenarios. Tidal flats are shown in grey.

https://doi.org/10.5194/os-2019-50
Preprint. Discussion started: 11 June 2019

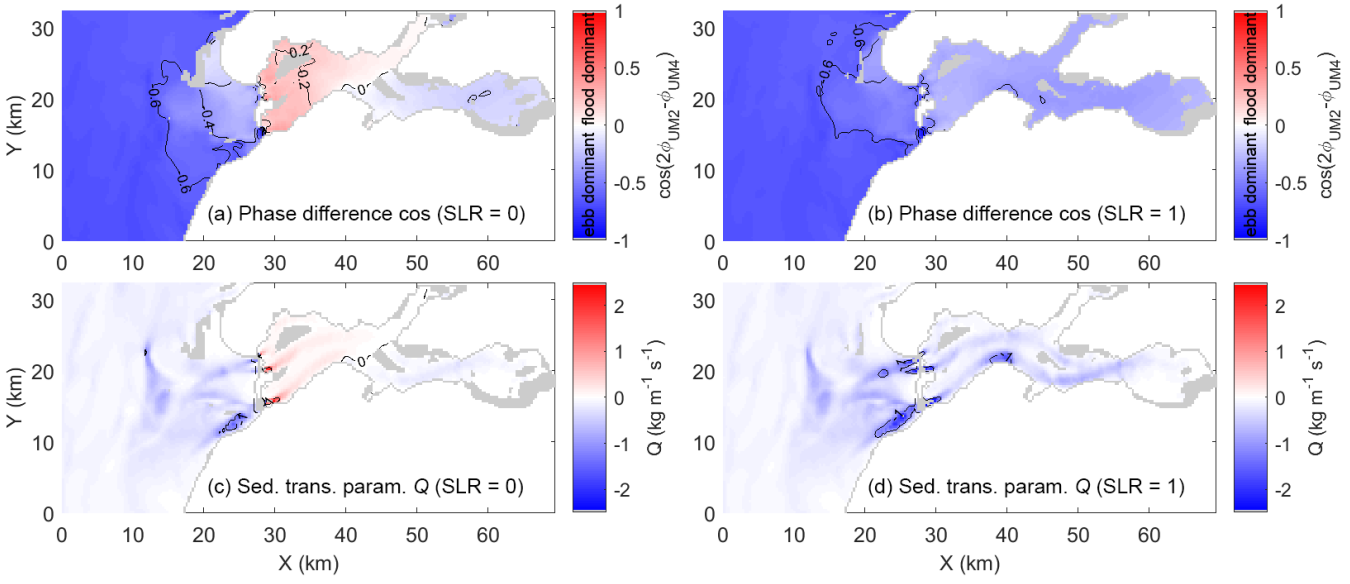

Figure 5: (a and b) cosine of M2-M4 velocity phase difference and (c and d) sediment transport quantity *Q* in the baseline and 1 m SLR scenarios. Positive (negative) *Q* denotes landward (seaward) transport. Tidal flats are shown in grey.

https://doi.org/10.5194/os-2019-50
Preprint. Discussion started: 11 June 2019

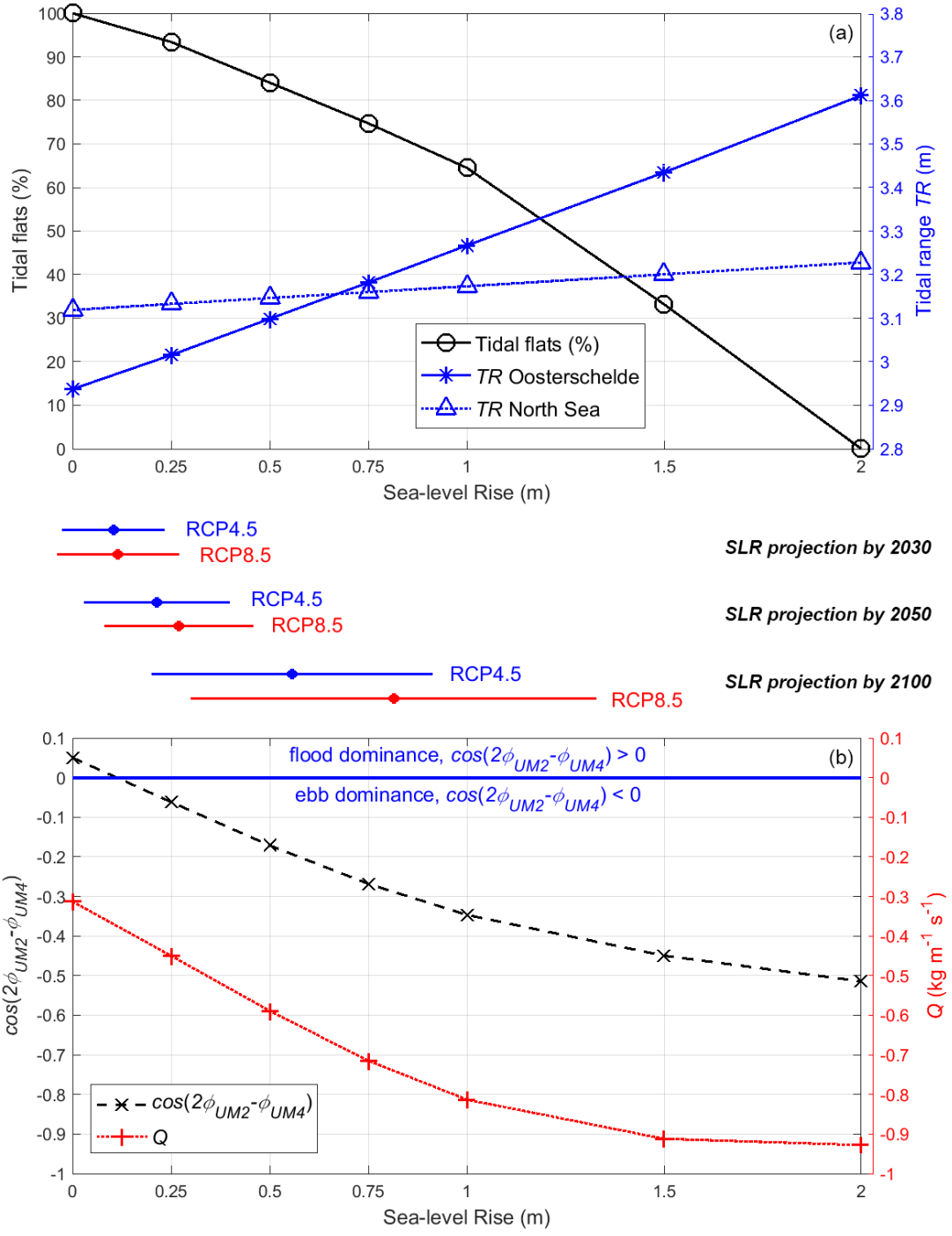

Figure 6: (a) Variations of the basin-average tidal flats percentage (defined as 100% in the baseline scenario) and average tidal range of the Eastern Scheldt (ES) and North Sea in the baseline and SLR scenarios; (b), same as (a), but for the cosine of M2-M4 velocity phase difference and sediment transport quantity *Q* averaged over ES. Scales between two panels are the local SLR projections (between the 5% and 95% confidence levels) in emission scenarios RCP4.5 and RCP8.5 in future decades, and dots on each scale denote projection medians.

https://doi.org/10.5194/os-2019-50
Preprint. Discussion started: 11 June 2019

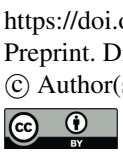

Ocean Science
Discussions
Open Access
EGU

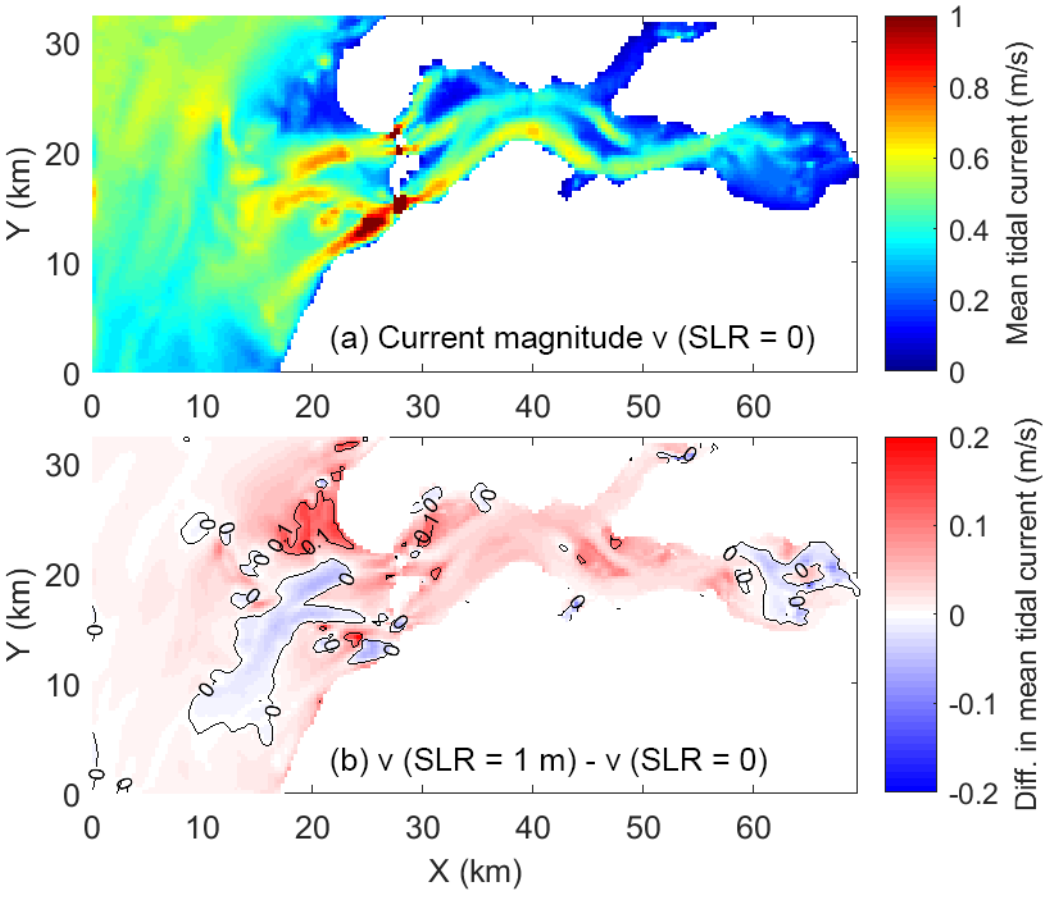

Figure 7: (a) The annual average magnitude of tidal currents in the baseline scenario and (b) the difference between the 1-m-SLR and baseline scenarios.

https://doi.org/10.5194/os-2019-50
Preprint. Discussion started: 11 June 2019

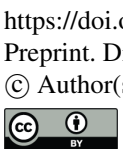

Ocean Science
Discussions
Open Access
EGU

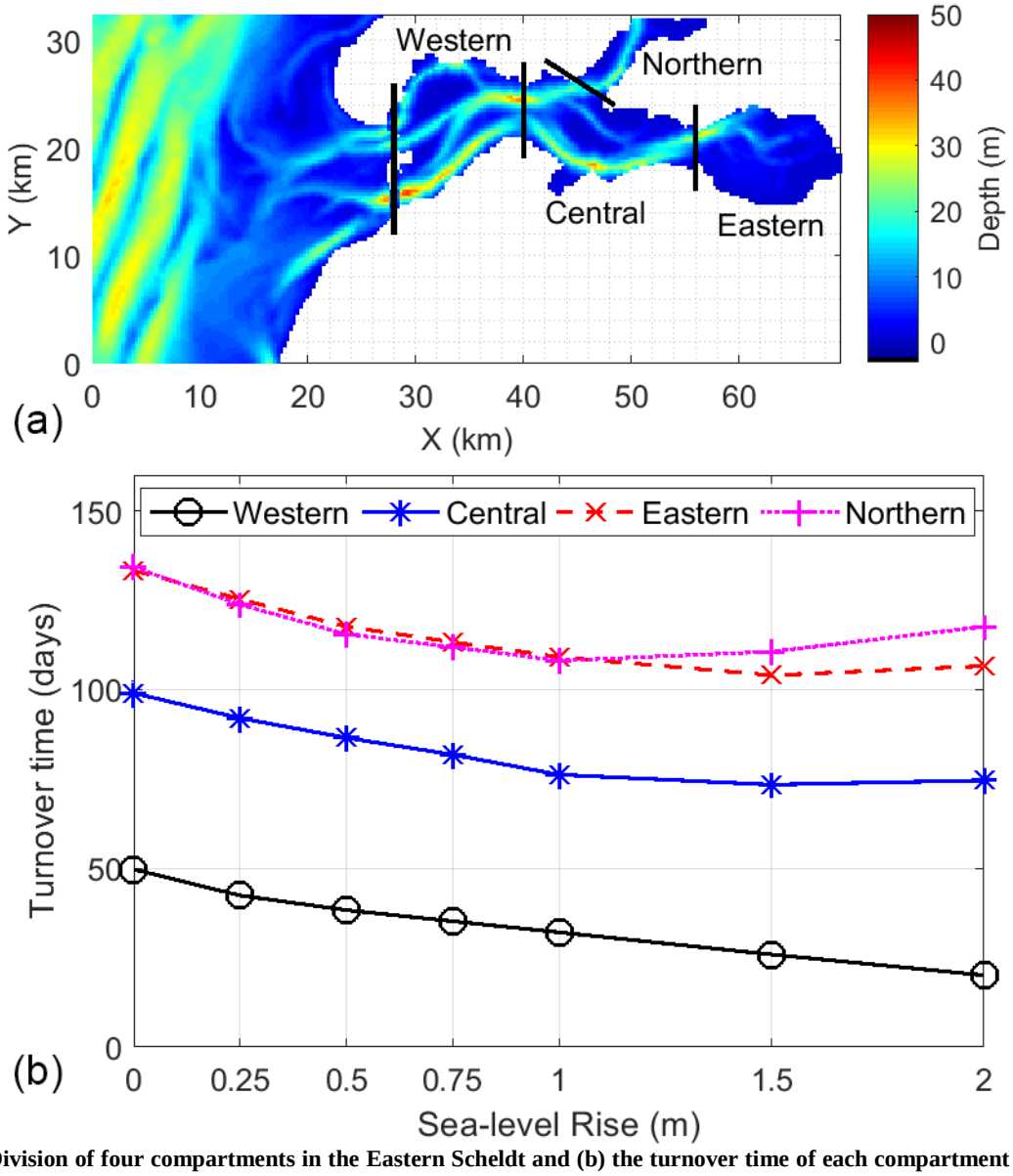

Figure 8: (a) Division of four compartments in the Eastern Scheldt and (b) the turnover time of each compartment in the baseline and SLR scenarios. The calculation of turnover time is detailed in Jiang et al., 2019.